Bismuth coatings deposited by the pulsed dc sputtering technique

M.F. Ortiz[a,b] J.J. Olaya[a,b], and J.E. Alfonso[*,b]
[a]*Departamento de Ingeniería Mecánica y Mecatrónica, Universidad Nacional de Colombia.*
[b]*Grupo de Ciencia de Materiales y Superficies, Departamento de Física, Universidad Nacional de Colombia,*
[*]*Tel: +57-1-3165000 ext. 13040*
e-mail: jealfonsoo@unal.edu.co

Received 31 August 2012; accepted 31 January 2013

In this work we present the results obtained from the deposition of nano-structured bismuth coatings through DC pulsed unbalanced magnetron sputtering. The coatings were grown on two substrates: silicon and AISI steel 316 L. The microstructure of the Bi coatings grown on silicon and the corrosion resistance of the Bi coatings grown on AISI steel were evaluated. The microstructure was evaluated by X-ray diffraction (XRD) and the corrosion resistance was characterized by means of polarization potentiodynamic and electrochemical impedance spectroscopy. Finally the morphology of the coatings was evaluated through scanning electronic microscopy (SEM). The XRD analysis indicates that the coatings are polycrystalline; the corrosion resistance tests indicate that the films with better corrosion resistance were deposited at 40 kHz. SEM micrographs show that the coatings are grown as granular form.

Keywords: Pulsed unbalanced magnetron sputtering; bismuth coatings; corrosion.

PACS: 81.15.Cd; 61.10.Nz; 68.37.-d; 81.65.Kn

1. Introduction

Some authors have recently reported that bismuth is a highly anisotropic semi-metal belonging to group V [1-2] with a rhombohedral A7 crystallinity structure (2 atoms per unit cell) which is typical of this group. This structure can be also described as a pseudocubic cell [3-4] with one atom per unit cell [5].

Moreover Bi exhibits thermal conductivity, about one order of magnitude lower than that of typical metals, a small density of states at the Fermi level [6], low carrier concentration and a small effective mass m* [7-8]. These properties allow it be used in various applications, such as thermoelectric conversion [9], devices exploiting large magneto-resistance [10] and reference electrodes used to detect heavy metals [11-12]. Another interesting property exhibited by Bi is the transformation of films of this semi-metal in to semiconductors at a critical thickness of approximately 30 nm [2,13]. These films can be deposited by different techniques such as laser pulsed deposition [1,14], RF and DC sputtering [15] and thermal evaporation [16].

Moreover, it is important to note that different authors have reported that when coatings are deposited through physical vapor deposition (PVD) techniques the crystalline structure and morphology of the Bi coatings depend on the deposition parameters such as: the temperature of the substrate [13], the potential applied to the target [17], the ion beam energy [18] and the rate at which energy is released when the films are deposited by ion beam bombardment [19-20]. In DC sputtering, these parameters can be affected by applying positive pulses between the substrate and the target [21]; this improves the film's density and mechanical properties [19,22-23]. Similar results have been reported about metallic coatings(see, *e.g.*, reference [24] for Al, Ti and reference [25] for Cu) and metalloid silicon targets [26] grown in an argon atmosphere.

In order to establish the potential electrochemical applications of Bi coatings, we have investigated the crystalline structure and corrosion resistance of Bi coatings as functions of the frequency applied through the pulsed DC sputtering technique.

2. Experimental details

Bismuth thin films were deposited simultaneously on [100] Si and AISI 316 L steel substrates using an unbalanced magnetron sputtering (UBM) instrument from Gencoa. The coatings on both substrates were obtained from a 4"$\times$1/4" Bi (99.99%) target in an Ar (99.999 %) atmosphere. The distance from the substrate to target was 50 mm. The base pressure in the deposition chamber was 8×10^{-4} Pa and the working pressure was 0.5 Pa with an Ar flow of 9 sccm. The discharge power for all samples was held constant at 68 W and the deposition parameter was pulsed frequencies of 0 kHz, 40 kHz and 80 kHz with the Bi thin films being deposited without intentional heating. The deposition time was adjusted to obtain a thickness of approximately 400 nm for all the Bi coatings.

The thickness of the coatings deposited on silicon was measured using a profilometer DEKTAK 150 at a displacement of 20 mm and an applied force of 1 mgf and their microstructure was investigated by X-ray diffraction (XRD) analysis. The coatings deposited on AISI stainless steel were tested for their corrosion resistance and their surface morphology before and after the corrosion tests was evaluated by scanning electronic microscopy (SEM).

The XRD analysis was carried out on an X-Pert Pro Panalytical instrument in the Bragg- Brentano configuration at a

current intensity of 40 mA, a voltage of 45 kV and by using the 1.5409 Å monochromatic line of Cu. The scanning angular range extending from 20° to 60° was covered in step size of 0.02° in continuous mode. The surface morphology of the Bi films was studied using a scanning electron microscope (XL 30 ESEM TMP) and micrographs were obtained using a mixture of secondary and backscattered electrons accelerated under a pressure of 10^{-4} Pa and at 30 kV. The corrosion resistance of the coatings was evaluated through polarization potentiodynamic and spectroscopy impedance studies using a three-electrode system in a Gamry 600 potentiostat. The substrates were placed at the working electrode, and a carbon rod was used as a counter electrode; a calomel saturated electrode was used as the reference electrode. The electrolyte used was composed of 8.5 g/l NaCl, 0.25 g/l KCl, 0.22 g/l $CaCl_2$, and 0.15 g/l $NaHCO_3$, with a pH value of 7.8±0.1 at room temperature and an exposed area of 0.196 cm^2. This mixture simulates a physiological saline solution.

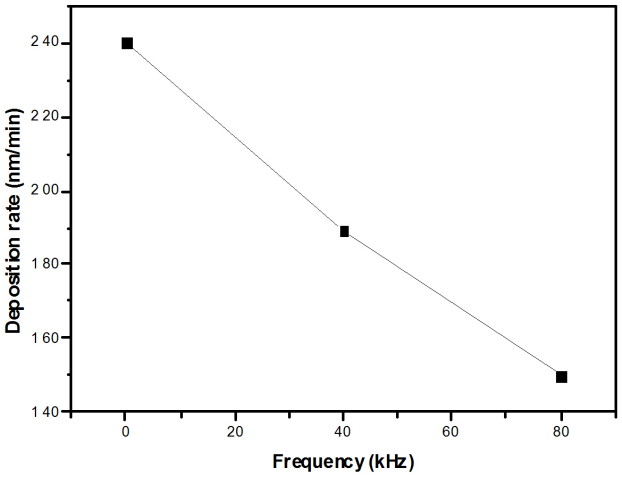

FIGURE 1. Deposition rate for each used frequency.

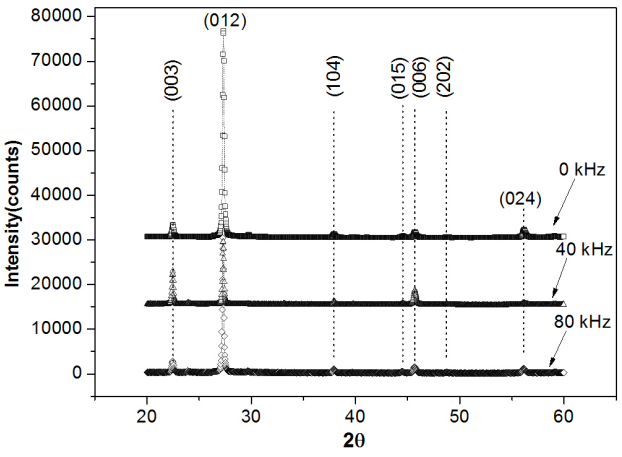

FIGURE 2. X-ray diffraction patterns of Bi coatings deposited on Si substrate at 0 kHz, 40 kHz and 80 kHz.

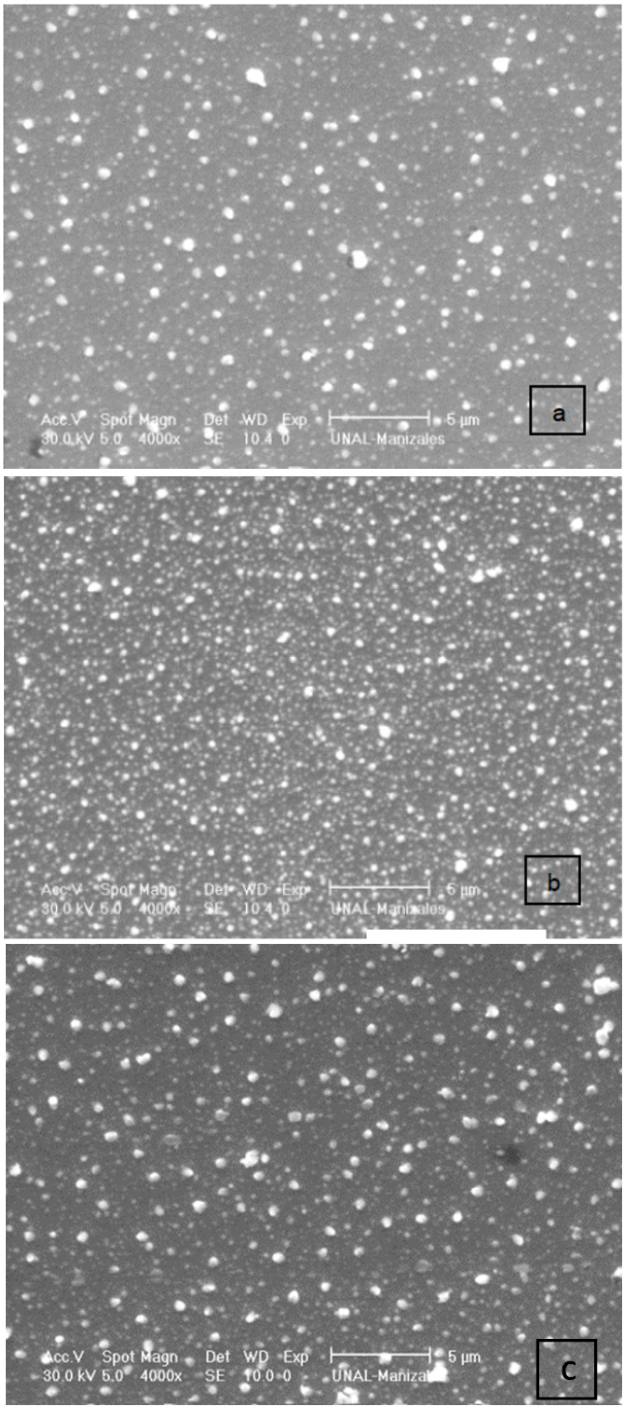

FIGURE 3. SEM micrograph of Bi film surface grown deposited on AlSi 316L at 0 kHz (a), 40 kHz (b) and 80 kHz (c).

3. Results and discussion

In order to study the influence of the pulse frequency on the surface morphology and the corrosion resistance, we deposited the Bi coatings on Si and stainless steel 316 substrates at different frequencies (0 kHz, 40 kHz and 80 kHz). Figure 1 gives the deposition rate versus frequency. The results indicate a strong decrease of this quantity with increasing fre-

quency. This could be due to the fact that the ion current density increases with the frequency generated dense plasma, which makes that both the mean free path and the probability that the electron reaches the substrate decrease [27].

Figure 2 shows the XRD pattern of the Bi films deposited on silicon substrate for different frequencies. In overall, the films were polycrystalline presenting peaks associated with the main planes (003), (012), (104), (015), (113), (202) and (024) that correspond to the rhombohedral phase (PDF 441246). Hence, the diffraction patterns of the bismuth films have the same polycrystalline behavior as the bulk Bi, although the relative intensities exhibit changes between different films according to the deposition conditions establishing the thermodynamic properties of the grown Bi films. Peaks associated with Bi_2O_3 were not found in the XRD patterns, indicating that the bismuth films were not oxidized.

The films showed a slight shift toward higher Bragg angles relative to the angles observed for the bulk material (JCPDS 441246), indicating the occurrence of stresses or slight lattice distortions. This may be mainly a consequence of the displacement of atoms to interstitial lattice places, because the ion energy exceeded the energy for atom displacement.

A SEM micrograph of the surfaces of the Bi coatings deposited at different frequencies is shown in Fig. 3. The images show a surface with a granular structure featuring densely packed grains [29].

Figure 4 shows the potentiodynamic polarization curves of Bi films grown on stainless steel. The corrosion resistance of a material is determined from a polarization curve by its ability to retain low current densities and positive potential corrosion. In this study, Bi films showed less corrosion resistance with respect to the AISI 316 L steel substrates. The barrier properties of the coatings depend on the microstructure, interfacial adhesion and residual stresses. For coatings deposited by physical vapor deposition (PVD), the inter-

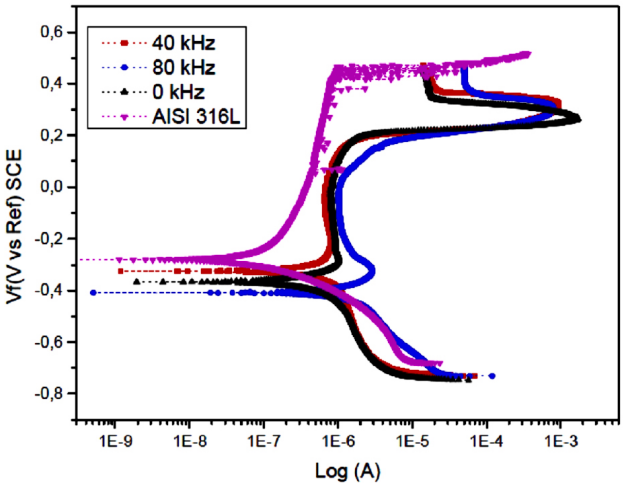

FIGURE 4. Potentiodynamic polarization results for the AlSi 316L substrate and Bi coatings deposited on it at frequencies of 0 kHz, 40 kHz and 80 kHz.

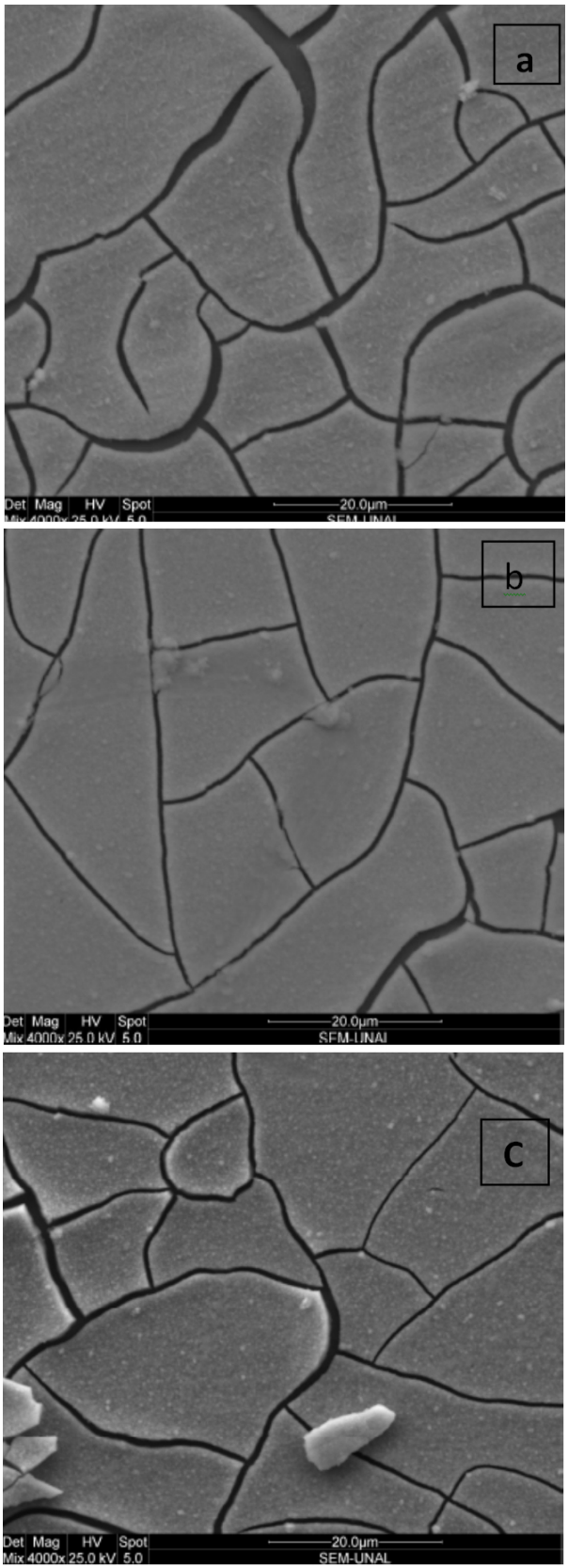

FIGURE 5. SEM micrographs of Bi films deposited on AlSi 316L at 0 kHz (a), 40 kHz (b) and 80 kHz (c) after potentiodynamic polarization.

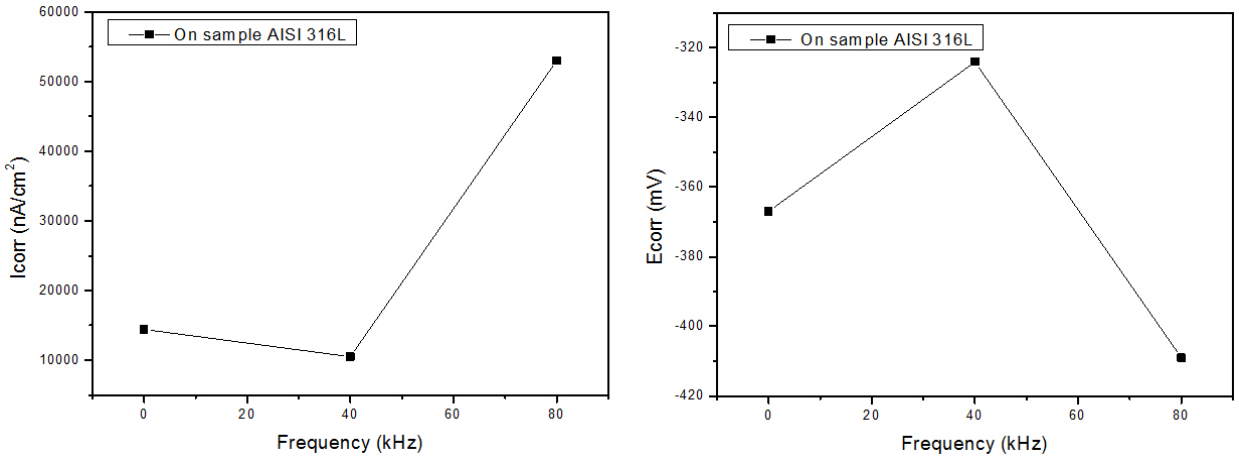

FIGURE 6. (a) Icorr and (b) Ecorr of bismuth coatings deposited on AISI 316L.

columnar space, micro and nano-pores (pinholes) and possible micro cracks allow for the diffusion of the electrolyte toward the substrate, leading to substrate corrosion and film delamination. In this study, the low corrosion resistance of the Bi coatings was clearly demonstrated by the low positive corrosion potential and high corrosion current measured. Figure 5 shows the typical blistering type delimitation of the Bi film, which was obtained after of polarization potentiodynamic. This phenomenon can be explained by the galvanic coupling produced by difference in the corrosion potential between the coating and the substrate. The potential difference is characterized by the anodic dissolution of the substrate material with a high anodic current density at the defect site, leading to the adhesion failure of the coating. Finally, in the anodic region, the jumps in current indicate film breaking

The resistance corrosion as a function of the frequency (Fig. 6) shows that the changed in the corrosion resistance was very small for the films and that the films deposited at 80 kHz showed less corrosion resistance; it this can be explained by the ion energy on the growth surface which enhances the residual stress and thereby reduces the adhesion of the film on steel.

Information about the processes occurring at the coating/solution and substrate/solution interfaces can be obtained using EIS. Impedance spectra were evaluated using an equivalent circuit (EC) consisting of a set of circuit elements (capacitors and resistors), representing the physical and electrical features of the electrochemical interfaces. A constant – phase element (CPE) of an ideal capacitor was introduced to achieve better fitting. The impedance of a CPE is expressed as follows [3]:

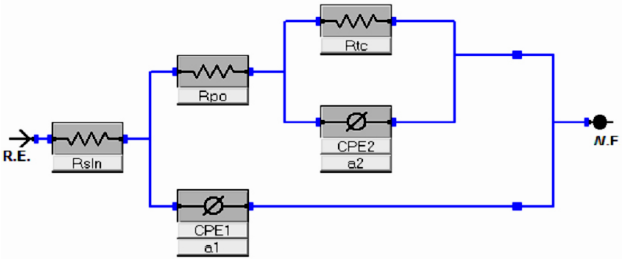

FIGURE 7. Equivalent circuit for bismuth film.

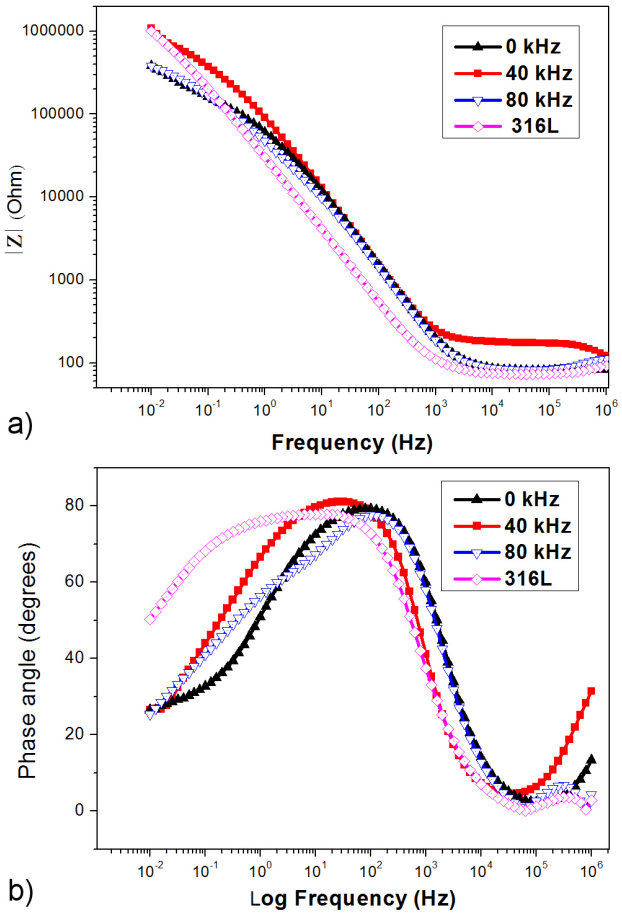

FIGURE 8. Bode plot the bismuth coating deposited on AISI 316L; a) Impedance vs. frequency, (b) phase angle vs. frequency.

$$z = Y_0^{-1}(jw)^{-\propto} \quad (1)$$

TABLE I. Simulation results of the one-hour electrical circuit test on bismuth coatings.

Frequency KHz	Rs	Rtc	Rpo	CPE2	a2	CPE1	a1
0	160,2	1,33E6	2,05E5	3,09E-6	5,51E-1	1,66E-6	9,33E-1
40	81,25	6,75E5	6,46E4	8,45E-6	5,10E-1	1,76E-6	9,23E-1
80	82,08	8,87E5	1,12E3	6,14E-6	4,82E-1	2,17E-6	9,75E-1
substrate AISI 316L	75,34	3,802E6	2,780E3	1,53E-6	4,68E-3	5,756E-6	8,97E-3

where Y_0 is the capacitance, ω is the angular frequency, j is an imaginary number and α represents capacitive value, where α = 1 indicates a perfect leak-free capacitor and a value between 0.5 and 1 indicates the existence of leaks, *i.e.*, the flow of electrons into the substrate. This value can be obtained from the slope of |Z| in a Bode plot.

Figure 7 presents the equivalent circuit model used to analyze the results of EIS for Bi films deposited on AISI 316 L steel. It consists of two RC' circuits connected in parallel, where CPE_1 represents the dielectric properties of the coatings and R_{po} represents the pore or the flow of current through the pores. The second phase constant CPE_2 and R_{tc} describe the process of charge transfer at the interface coating-substrate due to pinholes and pores. Meanwhile, R_{sln} represents the resistance of the electrolyte between the working electrode and the reference electrode. In this circuit, the relaxation time at higher frequencies represents the dielectric behavior of the coatings (CPE_1 and a_1) and the relaxation time at lower frequencies represents the properties of the substrate/coating interface (CPE_2 and a_2).

The EIS data given in Table I shows that Rtc decrease in the following order: un-coated substrate and Bi coated samples; also, the CPE_1 increased in the Bi films with the increase in the discharge frequency, indicating an inhomogeneous surface. The increase in the frequency (80 kHz) possibly increases the area of the pores, allowing for greater penetration of the corrosive solution toward the steel, producing localized corrosion. In-homogeneities are introduced by the surface roughness and porosities of the coatings, see Fig. 5. The electrolyte can diffuse through the pores and affect the substrate. The presence of a few micro-pores in the coatings resulted in a decrease in the coating capacitance and an increase in the charge transfer resistance of the pores. However, no significant variations in the CPE_1 of the coatings relative to the CPE_1 of the steel substrate were observed. This indicates that the surfaces of the coatings were more strongly affected, and for short immersion periods, the density of the corrosion products is low. As shown in Fig. 8, the shape of the Bode plot was similar for all of the coatings, indicating that the same corrosion mechanism occurs in all of the coatings.

4. Conclusion

In this study, we have successfully produced bismuth coatings using the pulsed DC unbalanced magnetron sputtering method. The following conclusions can be drawn from the obtained results:

Under the used experimental conditions, the depositions of the Bi films are characterized by an increase in the deposition rate as a function frequency and have a rhombohedral structure and granular morphology.

The Bi coatings obtained at 40 kHz show an increase in the corrosion resistance compared with those deposited at 0 and 80 kHz.

Electrochemical techniques, potentiodynamic and EIS, confirm that the bismuth coatings exhibited lower corrosion resistance than the stainless steel AISI 316 L substrate.

Acknowledgements

This research was carried out with financial support from Bisnano and the Direction the Investigation of Universidad Nacional de Colombia, sede Bogotá (DIB) through project No 203010016843.

1. M. O. Boffoué, B. Lenoir, H. Scherrer, and A. Dauscher, *Thin Solid Films* **322** (1998) 132-137.
2. H. Hattab, *et al*., *Thin Solid Films* **516** (2008) 8227-8231.
3. J. Chang, H. Kim, J. Han, M. H. Jeon, and W. Y. Lee, *J Appl Phys* **98** (2005) 023906.
4. P. M. Vereecken, L. Sun, P. C. Searson, M. Tanase, D. H. Reich, and C. L. Chien, *J Appl Phys* **88** (2000) 6529-6535.
5. H. Ph, *Progress in Surface Science* **81** (2006) 191-245.
6. H. Mönig, *et al*., *Phys. Rev B* **72** (2005) 085410.
7. C. R. Ast, and H. Höchst, *Phys. Rev Letters* **87** (2001) 177602.
8. T. Hirahara, T. Nagao, I. Matsuda, G. Bihlmayer, E. V. Chulkov, Y. M. Koroteev, and S. Hasegawa, *Phys. Rev B* **75** (2007) 035422.
9. D. H. Kim, S. H. Lee, J. K. Kim, and G. H. Lee, *Appl. Surf. Sci* **252** (2006), 3525-3531.

10. J. H. Mangez, J. P. Issi, and J. Heremans, *Phys. Rev B* **14** (1976) 4381-4385.

11. E. A. Hutton, B. Ogorevc, S. B. Hoèevar, F. Weldon, M. R. Smyth, and J. Wang, *Electrochem. Commun.* **3** (2001) 707-711.

12. R., Pauliukaite, S. B. Hoèevar, B. Ogorevc, and J. Wang, *Electroanalysis* **16** (2004) 719-723.

13. A. Jacquot, M. O. Boffoué, B. Lenoir, and A. Dauscher, *Appl. Surf. Sci* **156** (2000) 169-176.

14. J. H. Hsu, H. X. Wang, and P. C. Kuo, *J. Mag. Magn. Mater.* **294** (2005) e99-e103.

15. L. Kumari, S.J. Lin, J.H. Lin, Y.R. Ma, P.C. Lee, and Y. Liou, *Appl. Surf. Sci* **253** (2007) 5931-5938.

16. A. Dauscher, M. O. Boffoué, B. Lenoir, R. Martin-Lopez, and H. Scherrer, *Appl. Surf. Sci* **138-139** (1999) 188-194.

17. C. A. Jeffrey, S. H. Zheng, E. Bohannan, D. A. Harrington, and S. Morin, *Surf. Sci.* **600** (2006) 95-105.

18. S. Mammeri, S. Ouichaoui, H. Ammi, and R. Zemih, *Nuclear Instruments and Methods in Physics Research Section B: Beam Interactions with Materials and Atoms* **268** (2010) 140-148.

19. R. D. Arnell, P. J. Kelly, and J. W. Bradley, *Surf Coat Technol* **188-189** 158-163.

20. P. J. Kelly, and R. D. Arnell, *J Vac Sci Technol* **17** (1999) 945-953.

21. J. W. Bradley, H. Bäcker, P. J. Kelly, and R. D. Arnell, *Surf Coat Technol* **135** (2001) 221-228.

22. S. Schiller, K. Goedicke, J. Reschke, V. Kirchhoff, S. Schneider, and F. Milde, *Pulsed magnetron sputter technology Surf Coat Technol* **61** (1993) 331-337.

23. J. Lin, J. J. Moore, B. Mishra, W. D. Sproul, and J. A. Rees, *Surf Coat Technol* **201** (2007) 4640-4652.

24. A. Belkind, A. Freilich, J. Lopez, Z. Zhao, W. Zhu, and K. Becker, *New Journal of Physics* **7** (2005) 90-90.

25. S. Karthikeyan, A. E. Hill, J. S. Cowpe, and R. D. Pilkington, *Vacuum* **85** (2010) 634-638.

26. M. J. Jung, Y. M. Jung, L. R. Shaginyan, and J. G. Han, *Thin Solid Films* **420-421** (2002) 429-432.

27. H. Bartzsch, P. Frach, and K. Goedicke, *Surf Coat Technol* **132** (2000) 244-250.

28. C. Kokkinos A. Economou, I. Raptis, C. E. Efstathiou, and T. N. Speliotis, *Electrochem. Commun.* **9** (2007) 2795-2800.

29. C. Kokkinos, and A. Economou, *Talanta* **84** (2011) 696-701.

30. J. O. A. M. U. Piratoba, *Revista Dyna.* **164** (2009).